

Published in final edited form as:

Acta Biomater. 2014 June ; 10(6): 2622–2629. doi:10.1016/j.actbio.2014.01.025.

## Synthesis and Characterization of CREKA-Conjugated Iron Oxide Nanoparticles for Hyperthermia Applications

Anastasia M. Kruse<sup>1</sup>, Samantha A. Meenach<sup>2</sup>, Kimberly W. Anderson<sup>1</sup>, and J. Zach Hilt<sup>1,\*</sup>

<sup>1</sup>Department of Chemical and Materials Engineering, University of Kentucky, Lexington, KY 40506 U.S.A.

<sup>2</sup>Department of Chemical Engineering, University of Rhode Island, Kingston, RI 02881 U.S.A

### Abstract

One of the current challenges in the systemic delivery of nanoparticles in cancer therapy applications is the lack of effective tumor localization. Iron oxide nanoparticles coated with crosslinked dextran were functionalized with the tumor homing peptide CREKA, which binds to fibrinogen complexes in the extracellular matrix of tumors. This allows for the homing of these nanoparticles to tumor tissue. The iron oxide nanoparticle core allows for particle heating upon exposure to an alternating magnetic field (AMF) while the dextran coating stabilizes the particles in suspension and decreases the cytotoxicity of the system. Magnetically mediated hyperthermia (MMH) allows for the heating of tumor tissue to increase the efficacy of traditional cancer treatments using the iron oxide nanoparticles. While MMH provides the opportunity for localized heating, this method is currently limited by the lack of particle penetration into tumor tissue, even after effective targeted delivery to the tumor site. The CREKA-conjugated nanoparticles presented were characterized for their size, stability, heating capabilities and biocompatibility. The particles had a hydrated diameter of 52 nm, were stable in PBS and media with 10% v/v FBS over at least twelve hours, and generated enough heat to raise solution temperatures well into the hyperthermia range (41 – 45 °C) when exposed to an AMF due to an average specific absorption rate (SAR) of 83.5 W/g. Cytotoxicity studies demonstrated that the particles have low cytotoxicity over long exposure times at low concentrations. A fibrinogen clotting assay was used to determine the binding affinity of CREKA-conjugated particles, which was significantly greater than the binding affinity of dextran, only coated iron oxide nanoparticles demonstrating the potential for this particle system to effectively home to a variety of tumor locations. Finally, it was shown that *in vitro* MMH increased the effects of cisplatin compared to cisplatin or MMH treatments alone.

---

© 2014 Acta Materialia Inc. Published by Elsevier Ltd. All rights reserved

\*Contact Author: J. Zach Hilt Associate Professor of Chemical Engineering Department of Chemical and Materials Engineering University of Kentucky 177 F. Paul Anderson Tower Lexington, KY 40506-0046 Tel.: +1-859-257-9844 Fax: +1-859-323-1929 hilt@engr.uky.edu.

**Publisher's Disclaimer:** This is a PDF file of an unedited manuscript that has been accepted for publication. As a service to our customers we are providing this early version of the manuscript. The manuscript will undergo copyediting, typesetting, and review of the resulting proof before it is published in its final citable form. Please note that during the production process errors may be discovered which could affect the content, and all legal disclaimers that apply to the journal pertain.

## Keywords

iron oxide nanoparticles; CREKA; fibrinogen; magnetically mediated hyperthermia

---

## 1. Introduction

Non-small cell lung cancer (NSCLC) is the leading cause of cancer-related deaths in the United States each year [1]. Survival without treatment for stage IV NSCLC is 6 months if left untreated and only 9 to 12 months with treatment. Hyperthermia, the heating of tissue to 41–45 °C, has been shown to be effective in treating lung cancer when used in conjunction with radiation or chemotherapy [2–4]. Current hyperthermia treatments (e.g., whole body and regional hyperthermia) have several disadvantages, including damaging healthy tissue, limited penetration of heat into the body, under-dosage of heat, and complications such as increased heart rate and increased cardiac output [5–7]. Hyperthermia treatments are further challenged by deep seated tumors and lack the ability to penetrate surrounding tissues to raise the tumor tissue into the hyperthermia range [8]. Although various limitations exist, treatment of cancer via hyperthermia in conjunction with cisplatin was shown to have synergistic effects [9] and sensitization of cisplatin-resistant cell lines [10]. Cisplatin (20 µg/mL or 200 µg/mL) combined with mild incubator-induced hyperthermia at 41 °C was shown to significantly decrease the surviving fraction of T24 bladder cancer cells *in vitro* [3]. In another study completed by Hettinga and coworkers, murine tumor cells were mutated *in vitro* for cisplatin resistance [10]. The cisplatin-resistant cell line was exposed to cisplatin (0 – 10 µg/mL) for 45 minutes at either 37 °C or 44 °C. Hyperthermia with cisplatin exposure resulted in a significant decrease in the percentage of cell survival of the cisplatin-resistant cells. A second experiment demonstrated that the cisplatin-resistant cells were sensitized by hyperthermia by pre-heating the cells at 44 °C for 10 minutes prior to 45 minutes of cisplatin exposure at 37 °C. This treatment sequence further decreased the cell survival of the cisplatin-resistant cells [10].

In the presence of an alternating magnetic field (AMF), iron oxide magnetic nanoparticles generate heat and can induce hyperthermia. Magnetically-mediated hyperthermia, which is the heating of tissue using heat generated by magnetic nanoparticles in the presence of an AMF, shows great promise in overcoming the limitations of current hyperthermia treatments due to the ability of nanoparticles to deliver heat directly to the tumor site, therefore limiting the heat exposure to surrounding tissues. Iron oxide nanoparticles (IONPs) have the ability to passively or actively target tumors, and in the presence of an external AMF, can generate heat via multiple possible loss mechanisms including Néel paramagnetic switching, friction losses from Brownian rotation, and hysteresis [8]. IONPs have been studied as imaging agents, drug delivery systems, and therapeutic enhancers due to their inherent biocompatibility, magnetic properties, and lack of protein adsorption after proper coating [11]. In cancer therapy applications of IONPs, the main limitation to treating solid tumors is the limitations of particle localization. Vascularization and the enhanced permeation and retention (EPR) effect allow for passive targeted delivery of nanoparticles to the periphery of solid tumors. However, active targeting through peptides or ligands can result in higher

local concentrations of nanoparticles and lower systemic concentrations, which is required for more effective treatment [12].

CREKA, a tumor homing peptide, recognizes fibrin-associated plasma proteins, which are overexpressed in cancerous tissue but not in normal, healthy tissue. The walls of tumor vessels and the interstitial space within tumors contain these fibrin-fibronectin complexes due to protein seepage from the leaky vasculature of the tumor [12]. It was shown that CREKA can specifically target fibrin-fibronectin complexes as demonstrated by the lack of the peptide targeting to syngeneic B16F1 melanoma tumors grown in mice null of fibrinogen or lacking plasma fibronectin but significant homing to syngeneic B16F1 melanoma tumors in wild-type mice of the same litter [13]. CREKA is a small, linear peptide of five amino acids, which makes it attractive to use for conjugation with nanoparticles since multiple peptides can be conjugated to a single nanoparticle [13]. IONPs do not require internalization into cancer cells to be effective at heating the tumor tissue. Internalization of IONPs has been shown to enhance the anti-cancer effects of thermal energy dissipation compared to bulk hyperthermia methods [14]. Intracellular hyperthermia does not result in a bulk temperature rise but rather relies on the ability of individual nanoparticles to raise the temperature of their immediate surroundings [15]. Although targeting promoted uptake of IONPs can enhance their intracellular concentration, the targeting peptides, such as EGFR, are still cell line specific. Therefore, CREKA conjugation to IONPs is advantageous over other peptides in that it binds to complexes within the tumor vasculature rather than specific integrins on the surface of cells [12].

In this study, peptide-conjugated dextran-coated IONPs for enhanced tumor homing have been developed and characterized. Physicochemical characterization and *in vitro* biocompatibility studies are imperative for rationally develop and understanding a nanoparticle system. Prior to *in vivo* studies, the properties of this nanoparticle system such as size, stability, heating profiles, toxicity, and fibrinogen binding affinity need to be optimized. The desired size range for our nanoparticles is around 50 nm, which is expected to allow for tumor penetration and initial accumulation to tumor tissue via the EPR effect. Stability in media is an important property for systemically delivered nanoparticles, and the heating properties must be sufficient to induce hyperthermia conditions upon exposure to an AMF with substantial SAR values. Nanoparticle systems used for biological applications such as these must be screened for toxicity at low concentrations over long time frames, and for this specific peptide-conjugated IONP system, the binding affinity of the particles to fibrinogen complexes was important to verify since fibrinogen complexes within the tumor vasculature are the target of this system. A proof-of-concept study was then completed to show that this nanoparticle system could be used to enhance the effectiveness of cisplatin through magnetically mediated hyperthermia. This peptide-conjugated IONP has optimal physical characteristics, such as size [16, 17] and stability, for tumor homing via fibrin-fibronectin complexes and heating capabilities, which can be utilized for the hyperthermia treatment of lung cancer, in combination with chemotherapy. Although this study focuses on CREKA-conjugated IONPs for the treatment of lung cancer, this nanoparticle system has the ability to treat a multitude of cancerous tumors since it

recognizes fibrinogen complexes rather than specific surface integrins, which are often cell line dependent.

## 2. Materials and Methods

### 2.1 Materials

Iron (III) chloride hexahydrate ( $\text{FeCl}_3 \cdot 6\text{H}_2\text{O}$ ), iron (II) chloride ( $\text{FeCl}_2 \cdot 4\text{H}_2\text{O}$ ), 9 – 11 kDa dextran, epichlorohydrin (ECH), cisplatin (CDDP), fibrinogen, di-methyl sulfoxide (DMSO), and thrombin were obtained from Sigma Aldrich (St. Louis, MO). Ammonium hydroxide ( $\text{NH}_4\text{OH}$ ) was purchased from EMD Chemicals (Gibbstown, NJ). N-[ $\alpha$ -methylmaleimidoacetoxyl]succinimide ester (AMAS) linker was obtained from Thermo Scientific (Rochester, NY). CREKA peptide conjugated with 5-FAM-aminohexanoic acid (FAM-CREKA) was custom ordered through Biomatik (Cambridge, Ontario). Fetal bovine serum (FBS) was purchased from Fisher Scientific (Florence, KY). Dulbecco's Modified Eagle Medium (DMEM), pen-strep, L-glutamine, Fungizone®, and sodium pyruvate were all purchased from Invitrogen (Grand Island, NY), and trypsin was purchased from American Type Culture Collection (ATCC, Manassas, VA). 190 proof ethanol was purchased from Pharmco-Aaper (Shelbyville, KY) and phosphate buffered saline solution (PBS) (10X) was purchased from EMD Millipore (Billerica, MA). All materials were used as received.

### 2.2 Crosslinked dextran coated iron oxide nanoparticle synthesis

A modified one-pot co-precipitation method [18] was used to prepare dextran coated IONPs.  $\text{FeCl}_3 \cdot 6\text{H}_2\text{O}$  and  $\text{FeCl}_2 \cdot 4\text{H}_2\text{O}$  were combined in a 2:1 molar ratio (2.2 grams and 0.8 grams, respectively) and dissolved in 25 mL deionized (DI) water and sealed in a three-neck flask under vigorous stirring and an inert nitrogen environment. 11 grams of dextran was solubilized in 50 mL of DI water and added to the three-neck flask. The solution was heated to 85 °C at which 5 ml of  $\text{NH}_4\text{OH}$  was injected into the vessel. The reaction was carried out for 1 hour at 85 °C. The particles were centrifuged at 1000 rpm for 10 minutes to remove large agglomerates. The remaining particles were then dialyzed against DI water for 24 hours. Dextran coated IONPs were crosslinked using ECH for increased stability [19]. The particle colloid (9 mL, 1 mmol Fe) was added to 9 mL 5M NaOH and 2 mL ECH. The reaction was carried out for 24 hours at room temperature under continuous agitation. The particles were then dialyzed against DI water for 24 hours to remove excess ECH. Crosslinked IONPs were then aminated to allow for peptide conjugation. This was accomplished by reacting 0.2 mL of 30% ammonium hydroxide with the particles (5 mL, 0.2 mmol Fe) for 24 hours at room temperature under continuous agitation. The particles were then dialyzed against DI water for 24 hours.

### 2.3 CREKA conjugation of iron oxide nanoparticles

Amine conjugated IONPs were further conjugated with AMAS (N-[ $\alpha$ -maleimidoacetoxyl]succinimide ester) linker. The primary amines on the nanoparticles react with the N-hydroxysuccinimide of the linker, and CREKA can then be conjugated to the particle surface by reacting the sulfhydryl group on the cysteine with the maleimide group of the linker. Particles were resuspended at a concentration of 1 mg Fe/mL in PBS, and 2.5 mg AMAS per 2 mg Fe were dissolved in DMSO prior to addition to the nanoparticle

suspension [13]. After the AMAS addition under vortexing, the reaction was carried out for 40 minutes at room temperature. Particles were then washed three times with PBS on 100,000 MWCO cellulose Millipore filtration columns. FAM-CREKA was then added to the particle suspension at 25 mg per 4 mg Fe [13]. Particles were incubated overnight at 4°C and then washed again with PBS. To serve as a control for the CREKA-conjugated IONPs, fluorescein isothiocyanate (FITC) was conjugated to amine groups on crosslinked dextran IONPs. FITC was added in a 1:10 molar ratio to iron oxide (0.434 mmol Fe<sub>3</sub>O<sub>4</sub> and 0.0434 mmol FITC) and dissolved in 5 mL ethanol. The reaction was carried out for six hours at room temperature. The particles were then washed with DI water and concentrated using ultrafiltration columns. A summary of the systems investigated is included in Table 1, and a schematic of the systems synthesized is included in Figure 1.

## 2.4 Particle characterization

**Transmission electron microscopy (TEM)**—TEM was completed using a JEOL 2010F system operating at 200 KeV. Iron oxide nanoparticles were diluted to 200 µg/mL Fe in DI water and then dried on carbon TEM grids prior to analysis.

**Ultraviolet (UV)-Visible spectroscopy**—The stability of the nanoparticles was analyzed using a CaryWin 50 probe UV-visible spectrophotometer. IONPs were diluted to 200 µg/mL Fe in PBS or DMEM with 10% FBS. Sample absorbance was read at 540 nm over 12 hours.

**Thermogravimetric analysis (TGA)**—TGA was used to quantify the mass percent of the iron oxide core in the particle systems using a Netzsch Instruments STA 449A system. Approximately 5 mg of particle sample was heated at a rate of 5 °/minute. At 100 °C, the sample was held isothermally for 20 minutes to vaporize residual water. The samples were heated at 5 °/minute until reaching 500 °C where they were held isothermally for an additional 20 minutes. The reported mass loss reported was the actual mass loss normalized to the initial sample mass after isothermal heating at 100 °C.

**Dynamic light scattering (DLS)**—DLS measurements were obtained using a Beckman Coulter Delsa Nano C particle analyzer. Nanoparticle solutions were diluted to 200 µg/mL and were sonicated in a water bath prior to size analysis.

**Alternating magnetic field (AMF) heating**—The nanoparticle heating profiles were obtained using a custom made Taylor Winfield magnetic induction source, and the temperature was measured with a fiber optic temperature sensor (Luxtron FOT Lab Kit from LumaSense). Nanoparticle suspensions were diluted in DI water to a concentration of 5 mg/ml iron oxide. One milliliter of suspension in a 2 ml microcentrifuge tube was placed in the center of the AMF induction coil. The suspension was heated at a field amplitude of 58 kA/m and frequency of 292 kHz until the temperature of the suspension reached steady-state. The specific absorption rate (SAR) values of the nanoparticle suspensions were then calculated using the following equation:

$$SAR = \frac{C_{p,Fe} m_{Fe} + C_{p,H_2O} m_{H_2O}}{m_{Fe}} \frac{dT}{dt} \quad [1]$$

where  $C_{p,Fe}$  is the heating capacity of iron,  $m_{Fe}$  the mass of iron,  $C_{p,H_2O}$  the heating capacity of water,  $m_{H_2O}$  the mass of water, and  $dT/dt$  the initial slope of the heating profile.

## 2.5 Cytotoxicity analysis of particle systems

A549 lung carcinoma cells obtained from ATCC were cultured from passages 5 – 10 in DMEM supplemented with 10% FBS, 10  $\mu\text{g/ml}$  Fungizone®, 2  $\mu\text{g/ml}$  penicillin-streptomycin, and 4mM L-glutamine. Cells were seeded into 96-well plates at 4,000 cells/well and incubated for 24 hours. The cells were then exposed to nanoparticles in complete cell media at concentrations of 50, 100, 350, and 500  $\mu\text{g Fe/ml}$ . Cytotoxicity was determined using a calcein red fluorescent stain (1  $\mu\text{M}$ ,  $\lambda_{ex}=540\text{nm}$  and  $\lambda_{em}=590\text{nm}$ ) after 24 and 48 hours. Cell viability was analyzed using a Biotek SynergyMx microplate reader and the fluorescence of the cells exposed to the nanoparticle solutions was normalized to the fluorescence of the control cells.

## 2.6 CREKA and CREKA IONP binding affinity to fibrinogen clots

To synthesize fibrinogen clots, 75  $\mu\text{L}$  of fibrinogen solution (2 mg/mL) in 0.9% NaCl was added to a 96-well plate. 30  $\mu\text{L}$  of a 2.5 U/mL thrombin solution in 0.9% NaCl was subsequently added to the same 96-well plates. The plates were placed in an incubator shaker at 37°C for 5 minutes, and then gels were formed after four hours incubation at 37°C. Binding affinity of fluorescently labeled CREKA conjugated IONPs (CREKA-IONP) was compared to the binding affinity of unconjugated CREKA (CREKA only) and FITC conjugated iron oxide nanoparticles without CREKA (FITC-IONP). CREKA-IONP and FITC-IONP systems were diluted by taking 5, 10, 25, and 50  $\mu\text{L}$  of nanoparticle solution and diluting to a total volume of 50  $\mu\text{L}$  with DI water. The exact nanoparticle concentration was not necessary due to taking the fluorescence ratio of the bound to free particles at the same concentration. CREKA was diluted to 50, 100, 250 and 500  $\mu\text{M}$ . 50  $\mu\text{L}$  of solution (particle or CREKA only) was added to each clot. After one hour, half of samples were washed twice with 120  $\mu\text{L}$  of DI water to remove any CREKA or IONPs not bound to the fibrinogen clots, and the fluorescence of the plate was read on the microplate reader ( $\lambda_{ex}=488\text{ nm}$  and  $\lambda_{em}=520\text{ nm}$ ). The bound CREKA or FITC fluorescence (washed gels) was normalized to the corresponding free (unwashed gels) solution for each sample.

## 2.7 In vitro magnetically mediated hyperthermia and cisplatin combined treatment

One mL of A549 lung carcinoma cells (passage 15) was suspended in complete cell culture media in a 1.5 ml microcentrifuge tube at a concentration of 300,000 cells. The vials were then centrifuged at  $800 \times g$  for 5 minutes to pellet the cells. The media supernatant was removed, and the cells were resuspended in 1 mL of the respective treatment solutions. The six treatments are outlined in Table 2. Cisplatin treatments were administered at 100  $\mu\text{M}$ , IONP were administered at a concentration of 3 mg/mL, and hyperthermia was induced by the presence of an alternating magnetic field (51–58 kA/m). Treatments lasted 30 minutes, and all controls were also exposed to experimental conditions (i.e. room temperature) for 30

minutes. After treatment, the vials were centrifuged at  $800 \times g$  for 5 minutes, the treatment solution was removed, and replaced with fresh media. A second centrifugation cycle was completed to further wash the cells of the treatment solutions. The treated cells were then seeded into 48-well plates at 30,000 cells/mL (250  $\mu$ L/well). The viability of the cells was analyzed 48 and 72 hours post-treatment using a calcein AM assay (2  $\mu$ M,  $\lambda_{ex}$ =494 nm and  $\lambda_{em}$ =517 nm) analyzed by a microplate reader. The fluorescence of the cells exposed to the various treatments was normalized to the fluorescence of the control cells at each time point. Additional analysis was completed to determine the type of effect MMH and cisplatin had on A549 cells after 72 hours using the following equations [9]: synergistic,  $[MMH + CDDP] < [MMH] \times [CDDP]/100$ ; additive,  $[MMH + CDDP] = [MMH] \times [CDDP]/100$ ; sub-additive,  $[MMH] \times [CDDP]/100 < [MMH + CDDP] < [MMH]$ ; if  $[MMH] < [CDDP]$ ; interference,  $[MMH] < [MMH + CDDP] < [CDDP]$ , if  $[MMH] < [CDDP]$ ; and antagonistic,  $[CDDP] < [MMH + CDDP]$ , if  $[MMH] < [CDDP]$ , where  $[MMH]$  represents the cell viability percentage exposed to magnetically mediated hyperthermia alone,  $[CDDP]$  represents the cell viability percentage exposed to cisplatin alone, and  $[MMH+CDDP]$  represents the cell viability percentage exposed to combined magnetically mediated hyperthermia and cisplatin.

## 2.8 Statistical analysis

Statistical analysis was completed using Daniel's XL Toolbox in Microsoft Excel. A 1-way ANOVA test was used to determine the statistical differences of the cytotoxicity analysis and magnetically mediated hyperthermia study. A student t-test was used to determine the statistical differences of the fibrinogen binding study.

## 3. Results and Discussion

### 3.1 Particle characterization

The iron oxide nanoparticles exhibited diameters of 5 – 13 nm as shown by the TEM images in Figure 2. The clustering of the iron oxide suggests that multiple cores are encapsulated by the dextran coating for each nanoparticle. Due to the low density (i.e., low contrast) of the dextran coating, no differences were observed between the TEM images of the  $Fe_3O_4+Dx$  and  $Fe_3O_4+Dx-ECH$  nanoparticles. As seen in Table 1, size analysis indicated that the number average hydrated diameters of the nanoparticle systems were approximately 52 nm. All polydispersity indexes were below 0.2 indicating uniform nanoparticle sizes. Particles of this size have been shown to extravasate into tumor tissue and have been used in passive tumor targeting by taking advantages of the leaky vasculature of the tumor and the enhanced permeation and retention effect [16, 17].

Ensuring the stability of nanoparticles in various types of solutions over time is very important, especially for the systemic delivery of therapeutics. Particle-particle interactions can induce aggregation and particle settling which can adversely affect the properties of the nanoparticles, such as heating capabilities and tumor targeting. Particle aggregates greater than 200 nm not only settle out of solution, but also attract opsonin proteins *in vivo* which label the particles for removal through the mononuclear phagocyte system (MPS)/reticuloendothelial system (RES) [17]. Using UV-visible spectroscopy, it was shown that the

nanoparticles were stable in both PBS and DMEM supplemented with 10% v/v FBS for each stage of particle synthesis over a time period of 12 hours (Figure 3), with the normalized absorbance indicating minimal to no particle settling in solution. Overall, these results indicate the high stability of the evaluated particle systems in multiple solutions.

Thermogravimetric analysis was used to confirm the presence of the dextran coating on the iron oxide nanoparticles. This showed that the coating accounted for 59 – 64% of the nanoparticle mass prior to CREKA conjugation. The coating weight percentage was calculated by subtracting the final mass fraction from the initial normalized mass. As depicted in Figure 4, crosslinking of the dextran coating with ECH was confirmed by the shift of the mass loss profile to the right where an increase in the temperature at which the greatest mass loss occurred shifted from 285 °C ( $\text{Fe}_3\text{O}_4+\text{Dx}$ ) to 306 °C, ( $\text{Fe}_3\text{O}_4+\text{Dx}-\text{ECH}$  and  $\text{Fe}_3\text{O}_4+\text{Dx}-\text{ECH}-\text{Amine}$ ), indicating a greater thermal stability of the coating. The observed single drop in particle mass with increasing temperature confirms a single dextran layer on the surface of the particles, as this abrupt change in weight has been previously associated with a monolayer of dextran [20]. The dextran coating of the final CREKA-IONP only accounted for 30% of the nanoparticle mass due to the dissolution of free dextran and AMAS linker in DMSO during the final CREKA conjugation process.

Dextran has a very high affinity for DMSO resulting in any free or weakly bound dextran solubilizing in the DMSO and being washed from the nanoparticle system during the washing process. As indicated by UV-visible spectroscopy, the CREKA-IONP remained stable in PBS and DMEM indicating that dextran was still present on the surface of the particles.

### 3.2 Remote controlled heating of iron oxide magnetic nanoparticles via AMF

In the presence of an AMF (58 kA/m, 292 kHz), the iron oxide nanoparticle systems (5 mg/mL  $\text{Fe}_3\text{O}_4$ ) heated the bulk solution into or above the hyperthermia range (41 – 45 °C) as seen in Figure 5.  $\text{Fe}_3\text{O}_4+\text{Dx}$ ,  $\text{Fe}_3\text{O}_4+\text{Dx}-\text{ECH}$ , and  $\text{Fe}_3\text{O}_4+\text{Dx}-\text{ECH}-\text{Amine}$  particles heated to 41 °C within 300 seconds. The final CREKA-IONP system took longer to reach the hyperthermia range and heated to a lower final temperature than the other systems. The iron concentration of the nanoparticles was determined using an iron assay prior to dilution for heating in the AMF except for the CREKA-IONP system. The exact iron concentration of the CREKA-IONP could not be determined due to low volume of particles so the initial iron concentration used in the synthesis of the CREKA-IONP was used. Therefore, if any iron oxide nanoparticles were lost in the ultracentrifugation washing steps post CREKA conjugation, the actual iron concentration of the AMF heating samples would be lower than calculated, accounting for the lower final temperature and decreased initial slope of the heating profile. The SAR values are reported in Table 1 and indicate the energy being produced per gram of iron oxide. The lower SAR value for the CREKA-IONP is accounted for by the previous explanation of the concentration discrepancy. The AMF amplitude and frequency correspond to a field frequency product of  $1.7 \times 10^{10} \text{A}/(\text{m}\cdot\text{s})$  which is significantly greater than the often quoted limit for use in humans [21]. The high field frequency product may be an issue for future use in humans, but, the cited value is only an estimation. There is a need for further studies to determine the effects of alternating



magnetic fields on healthy tissues in order to more accurately determine the limitations of AMF exposure [22].

### 3.3 Cytotoxicity analysis of particles

The cytotoxicity of the particles produced in each step in the particle synthesis was evaluated using A549 lung carcinoma cells. A549 cells were exposed to low doses of iron oxide nanoparticles for 24 and 48 hours, and the viability of the cells was analyzed using a calcein AM stain. As depicted in Figure 6, the particles exhibited no toxicity (at least 100% viability) after 24 hours. Dextran is a hydrophilic, water-soluble polymer which is inert in biological systems, therefore decreasing protein adsorption to the nanoparticle surface which would lead to toxicity [23]. After 48 hours, the particles were still mostly non-toxic at these concentrations, but there was a significant difference between the control and the CREKA-IONP at 100, 350, and 500  $\mu\text{g Fe/mL}$  as determined via a 1-way ANOVA test. However, the viability of the A549 cells after exposure to these concentrations for 48 hours is still above 80%, indicating that the particles are minimally toxic even though the difference from the control is significant.

### 3.4 Fibrinogen binding affinity

CREKA-IONPs were shown to bind to fibrin clots with a significantly greater bound-to-free fluorescence ratio than fluorescently tagged iron oxide nanoparticles (FITC-IONP) (Table 2). The bound-to-free fluorescence ratios of free CREKA and CREKA-IONPs were not significantly different, indicating that conjugation to the nanoparticle surface does not inhibit the binding properties of CREKA. The sulfhydryl group on the cysteine of CREKA is not required for binding to fibrinogen clots. Therefore, conjugation to the nanoparticle surface through a Michael addition reaction with an AMAS linker does not influence the fibrinogen binding properties of CREKA. These results indicate that CREKA can be functionalized to the IONP in order to localize the nanoparticles at the tumor site through binding with fibrinogen complexes in the extracellular matrix. CREKA-IONPs do not bind to specific integrins on the cell surface providing the opportunity to target a wider range of cancers. Additionally, CREKA-IONPs have resulted in amplified homing by inducing localized tumor clotting *in vivo* [13]. These clots then attract more CREKA-IONPs, and the cycle continues. This amplified homing of CREKA to the fibrin complexes within the tumor make it attractive for localizing high concentrations of IONPs at the tumor site for magnetically mediated hyperthermia.

### 3.5 Magnetically-mediated hyperthermia

The heating properties of the magnetic iron oxide nanoparticles were utilized to induce *in vitro* hyperthermia conditions on A549 lung carcinoma, and the effects of combined MMH and cisplatin treatments were evaluated since cisplatin is known to increase MMH efficacy at elevated temperatures [4, 24]. Five treatments plus a control were evaluated as seen in Table 2 and cell viability 48 and 72 hours post-treatment was determined to allow time for cellular response to the treatments. After 48 hours (Figure 7), there is no significant difference between MMH treatment alone and combined cisplatin and MMH treatment (CDDP+MMH). However, at this time point there is also no difference between the viability

of cells exposed to cisplatin and the control, indicating that the cells have not responded to the cisplatin treatment. As seen in Figure 8, after 72 hours there is a significant difference ( $p < 0.01$ ) between the viability of cells exposed to MMH treatment alone and combined cisplatin and MMH treatment (CDDP+MMH). At this time point, the cells have responded to the cisplatin treatment, as shown by the significantly decreased viability of cells exposed to cisplatin compared to the control. Additionally, cell morphology dramatically changes when the cells are treated with cisplatin combined with MMH compared to either treatment alone. Images in Figures 7 and 8, show the cell with blebs, or localized decoupling of the cytoskeleton from the cell membrane, which is an indicator of apoptosis, or programmed cell death [25]. Therefore, cisplatin combined with MMH has a significantly greater effect on cell viability than either treatment alone.

The type of effect induced by the combined MMH and CDDP treatment was analyzed using the equations outlined in section 2.7. Seventy-two hours after treatment, the percent viability of the combined treatment was  $23.7 \pm 2.9$  and  $[\text{MMH}] \times [\text{CDDP}]/100$  equaled  $26.2 \pm 2.1$ , where the error represents standard error ( $n = 12$ ). Therefore, the combined treatment of hyperthermia and cisplatin was determined to be additive since these values are not significantly different, as indicated by a student t-test. This analysis was not completed on the 48 hour post-treatment data due to the cell viability of cisplatin only treatment not being different from the control.

There are several theories as to how the effects of cisplatin are enhanced by hyperthermia. Cisplatin operates by binding to DNA forming inter- or intra-strand crosslinks and interfering with the transcription DNA for protein synthesis, therefore preventing cell division, ultimately leading to cell death [26]. *In vitro* studies have shown that hyperthermia increases the intracellular concentration of cisplatin [27, 28] due to increased permeability of the cell membrane [24]. Therefore, the number of DNA-cisplatin crosslinks is also increased [29]. Additionally, inhibition of cellular resistance to cisplatin has been observed when combined with hyperthermia [30]. For *in vivo*, hyperthermia results in increased blood flow and vascular permeability allowing for greater drug uptake and improved oxygenation of the tumor tissue [5]. Hyperthermia has been shown to promote cell death by increasing the fluidity of membranes causing adverse intracellular and surface events, inactivating microtubule processes and by enhancing cellular antigen expression or antigen antibody complexation [31]. The efficacy of hyperthermia alone is not enough to replace any of the current chemotherapy standards, but its effects are sufficient to enhance the toxic effects of many chemotherapeutics. Therefore, by combining magnetically mediated hyperthermia and cisplatin, the effective dosage of cisplatin can be decreased, and therefore potentially decreasing the toxic side effects of the chemotherapeutic.

#### 4. Conclusion

CREKA-conjugated dextran coated iron oxide nanoparticles were successfully developed and characterized for their use in targeted hyperthermia applications. The nanoparticles have properties suitable for systemic tumor targeting through the enhanced permeation and retention effect such as stability in cell culture media and a size of approximately 50 nm [16, 17]. In the presence of an alternating magnetic field, the particles generated sufficient heat to

increase the bulk solution temperature into the hyperthermia range. CREKA-conjugated nanoparticles were shown to bind to fibrinogen clots with a higher affinity than FITC-conjugated iron oxide nanoparticles, suggesting that the nanoparticles can be effective at targeting fibrinogen overexpressed in tumor tissues. The binding affinity of CREKA was not inhibited by conjugation to the iron oxide nanoparticles as shown by similar bound-to-free ratios of fluorescence. Low concentrations of the nanoparticle systems were non-toxic over long periods of time, indicating that the particles can be used for biological applications. When magnetically mediated hyperthermia was administered in conjunction with cisplatin, an enhanced cytotoxic effect was observed compared to cisplatin or hyperthermia alone. This peptide-conjugated nanoparticle system can be further studied to assess its ability to localize at tumor sites at sufficient concentrations to induce hyperthermia conditions upon exposure to an external alternating magnetic field.

## 5. References

- [1]. ACS. Cancer Facts and Figures. American Cancer Society; 2013.
- [2]. Vertrees RA, Das GC, Popov VL, Coscio AM, Goodwin TJ, Logrono R, et al. Synergistic Interaction of Hyperthermia and Gemcitabine in Lung Cancer. *Cancer Biology & Therapy*. 2005; 4:1144–53. [PubMed: 16138007]
- [3]. Itoh Y, Yamada Y, Kazaoka Y, Ishiguchi T, Honda N. Combination of chemotherapy and mild hyperthermia enhances the anti-tumor effects of cisplatin and adriamycin in human bladder cancer T24 cells in vitro. *Experimental and Therapeutic Medicine*. 2010; 1:319–23.
- [4]. Lee JS, Rodriguez-Luccioni HL, Mendez J, Sood AK, Lopez-Berestein G, Rinaldi C, et al. Hyperthermia Induced by Magnetic Nanoparticles Improves the Effectiveness of the Anticancer Drug cis-Diamminedichloroplatinum. *Journal of Nanoscience and Nanotechnology*. 2011; 11:4153–7. [PubMed: 21780419]
- [5]. Issels RD. Hyperthermia adds to chemotherapy. *European Journal of Cancer*. 2008; 44:2546–54. [PubMed: 18789678]
- [6]. Zwischenberger JB, Vertrees RA, Bedell EA, McQuitty CK, Chernin JM, Woodson LC. Percutaneous Venovenous Perfusion-Induced Systemic Hyperthermia for Lung Cancer: A Phase I Safety Study. *Annals of Thoracic Surgery*. 2004; 77:1916–25. [PubMed: 15172236]
- [7]. Kumar CSSR, Mohammad F. Magnetic nanomaterials for hyperthermia-based therapy and controlled drug delivery. *Advanced Drug Delivery Reviews*. 2011; 63:789–808. [PubMed: 21447363]
- [8]. Dennis CL, Jackson AJ, Borchers JA, Hoopes PJ, Strawbridge R, Foreman AR, et al. Nearly complete regression of tumors via collective behavior of magnetic nanoparticles in hyperthermia. *Nanotechnology*. 2009; 20:395103. [PubMed: 19726837]
- [9]. Babincova M, Altanerova V, Altaner C, Bergemann C, Babinec P. In vitro analysis of cisplatin functionalized magnetic nanoparticles in combined cancer chemotherapy and electromagnetic hyperthermia. *Ieee Transactions on Nanobioscience*. 2008; 7:15–9. [PubMed: 18334449]
- [10]. Hettinga JVE, Lemstra W, Devries EGE, Konings AWT, Kampinga HH. SENSITIZATION TO CISPLATIN ACTION BY STEP-DOWN HEATING IN CDDP-SENSITIVE AND CDDP-RESISTANT CELLS. *International Journal of Cancer*. 1995; 61:722–6.
- [11]. Laurent S, Dutz S, Hafeli UO, Mahmoudi M. Magnetic fluid hyperthermia: Focus on superparamagnetic iron oxide nanoparticles. *Advances in Colloid and Interface Science*. 2011; 166:8–23. [PubMed: 21601820]
- [12]. Ruoslahti E, Bhatia SN, Sailor MJ. Targeting of drugs and nanoparticles to tumors. *JCB: Review*. 2010; 188:759–68.
- [13]. Simberg D, Duza T, Park JH, Essler M, Pilch J, Zhang L, et al. Biomimetic amplification of nanoparticle homing to tumors. *Proceedings of the National Academy of Sciences*. 2007; 104:932–6.

- [14]. Creixell M, Bohorquez AC, Torres-Lugo M, Rinaldi C. EGFR-Targeted Magnetic Nanoparticle Heaters Kill Cancer Cells without a Perceptible Temperature Rise. *ACS Nano*. 2011; 5:7124–9. [PubMed: 21838221]
- [15]. Krpetic Z, Nativo P, See V, Prior IA, Brust M, Volk M. Inflicting Controlled Nonthermal Damage to Subcellular Structures by Laser-Activated Gold Nanoparticles. *Nano Lett*. 2010; 10:4549–54. [PubMed: 20923168]
- [16]. Phillips MA, Gran ML, Peppas NA. Targeted nanodelivery of drugs and diagnostics. *Nano Today*. 2010; 5:143–59. [PubMed: 20543895]
- [17]. Fox ME, Szoka FC, Frechet JMJ. Soluble Polymer Carriers for the Treatment of Cancer: The Importance of Molecular Architecture. *Accounts of Chemical Research*. 2009; 42:1141–51. [PubMed: 19555070]
- [18]. Frimpong RA, Dou J, Pechan M, Hilt JZ. Enhancing remote controlled heating characteristics in hydrophilic magnetite nanoparticles via facile co-precipitation. *Journal of Magnetism and Magnetic Materials*. 2010; 322:326–31.
- [19]. Stephen Palmacci, LJ. Synthesis of polysaccharide covered superparamagnetic oxide colloids. *Magnetics, A.*, editor. United States: 1993.
- [20]. Bautista MC, Bomati-Miguel O, Morales MD, Serna CJ, Veintemillas-Verdaguer S. Surface characterisation of dextran-coated iron oxide nanoparticles prepared by laser pyrolysis and coprecipitation. *Journal of Magnetism and Magnetic Materials*. 2005; 293:20–7.
- [21]. Atkinson WJ, Brezovich IA, Chakraborty DP. USABLE FREQUENCIES IN HYPERTHERMIA WITH THERMAL SEEDS. *Ieee Transactions on Biomedical Engineering*. 1984; 31:70–5. [PubMed: 6724612]
- [22]. Kozissnik B, Bohorquez AC, Dobson J, Rinaldi C. Magnetic fluid hyperthermia: Advances, challenges, and opportunity. *Int J Hyperthermia*. 2013; 29:706–14. [PubMed: 24106927]
- [23]. Imren D, Gumusderelioglu M, Guner A. Synthesis and characterization of dextran hydrogels prepared with chlor- and nitrogen-containing crosslinkers. *Journal of Applied Polymer Science*. 2006; 102:4213–21.
- [24]. Alvarez-Berrios MP, Castillo A, Mendez J, Soto O, Rinaldi C, Torres-Lugo M. Hyperthermic potentiation of cisplatin by magnetic nanoparticle heaters is correlated with an increase in cell membrane fluidity. *International Journal of Nanomedicine*. 2013; 8:1003–13. [PubMed: 23493492]
- [25]. Charras GT, Coughlin M, Mitchison TJ, Mahadevan L. Life and times of a cellular bleb. *Biophysical Journal*. 2008; 94:1836–53. [PubMed: 17921219]
- [26]. Butour J-L, Alvinerie P, Souchard J-P, Colson P, Houssier C, Johnson NP. Effect of the amine non-leaving group on the structure and stability of DNA complexes with cis-[Pt(R-NH<sub>2</sub>)<sub>2</sub>(NO<sub>3</sub>)<sub>2</sub>]. *European Journal of Biochemistry*. 1991; 202:975–80. [PubMed: 1765105]
- [27]. Takahashi I, Emi Y, Hasuda S, Kakeji Y, Maehara Y, Sugimachi K. Clinical application of hyperthermia combined with anticancer drugs for the treatment of solid tumors. *Surgery*. 2002; 131:S78–S84. [PubMed: 11821791]
- [28]. Ohno S, Siddik ZH, Kido Y, Zwelling LA, Bull JMC. THERMAL ENHANCEMENT OF DRUG UPTAKE AND DNA-ADDUCTS AS A POSSIBLE MECHANISM FOR THE EFFECT OF SEQUENCING HYPERTHERMIA ON CISPLATIN-INDUCED CYTOTOXICITY IN L1210 CELLS. *Cancer Chemotherapy and Pharmacology*. 1994; 34:302–6. [PubMed: 8033297]
- [29]. Meyn RE, Corry PM, Fletcher SE, Demetriades M. THERMAL ENHANCEMENT OF DNA DAMAGE IN MAMMALIAN-CELLS TREATED WITH CIS-DIAMMINEDICHLOROPLATINUM(II). *Cancer Res*. 1980; 40:1136–9. [PubMed: 7188882]
- [30]. Hettinga JVE, Lemstra W, Meijer C, Dam WA, Uges DRA, Konings AWT, et al. Mechanism of hyperthermic potentiation of cisplatin action in cisplatin-sensitive and -resistant tumour cells. *British Journal of Cancer*. 1997; 75:1735–43. [PubMed: 9192975]
- [31]. Hetzel FW, Dunn JA. Hyperthermia and radiation in cancer therapy: a review. *Radiat Phys Chem*. 1984; 24:337–45.

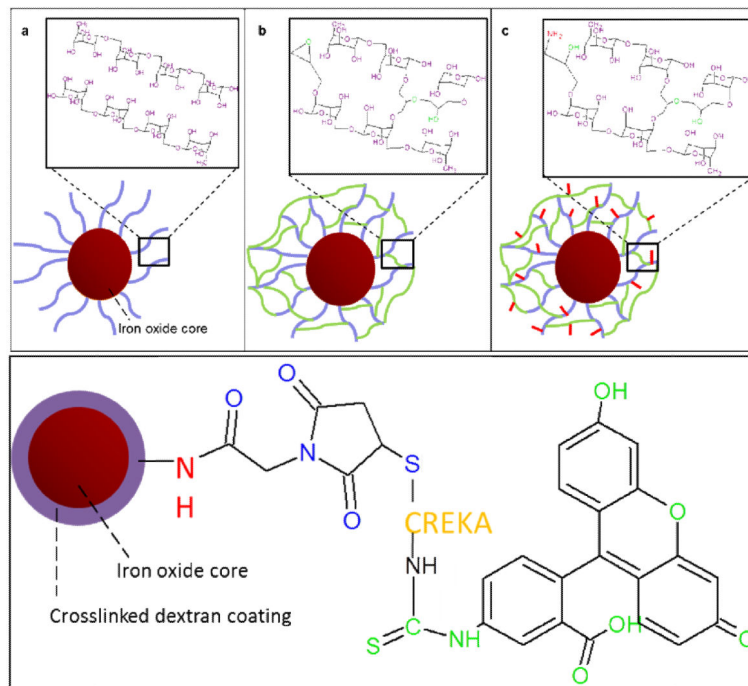


**Figure 1.**

Iron oxide nanoparticle synthesis process for the (a) dextran coating, (b) epichlorohydrin crosslinking, (c) amine conjugation, and (d) conjugated with and AMAS linker, connecting the FAM-labeled CREKA to the primary amine.

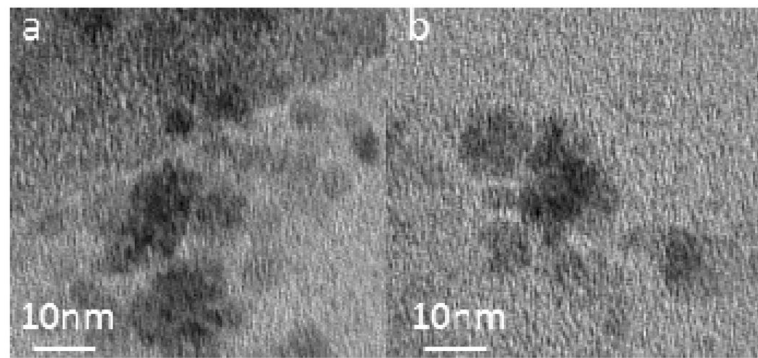


**Figure 2.**

TEM images of (a) dextran coated iron oxide nanoparticles ( $\text{Fe}_3\text{O}_4+\text{Dx}$ ) and (b) dextran-epichlorohydrin crosslinked iron oxide nanoparticles ( $\text{Fe}_3\text{O}_4+\text{Dx-ECH}$ ).

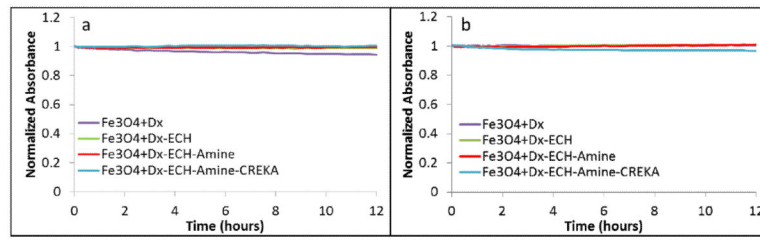


**Figure 3.**

Normalized absorbance (at 540 nm) of the iron oxide nanoparticle systems in (a) PBS and (b) DMEM with 10% v/v FBS over 12 hours using UV-visible spectroscopy.

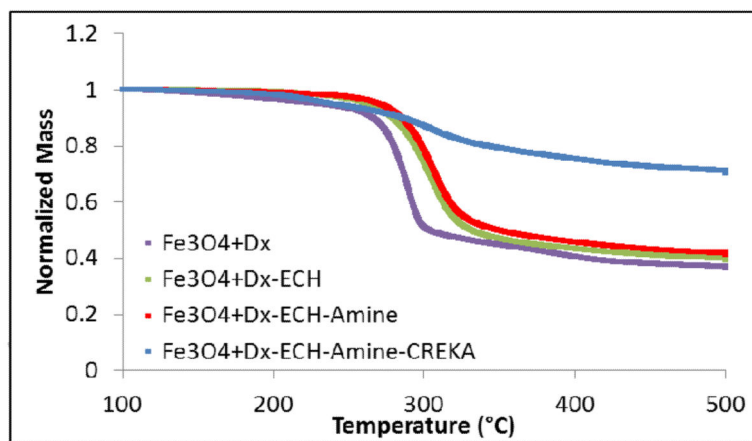


**Figure 4.**

Normalized mass loss of each nanoparticle system in the synthesis process via TGA.



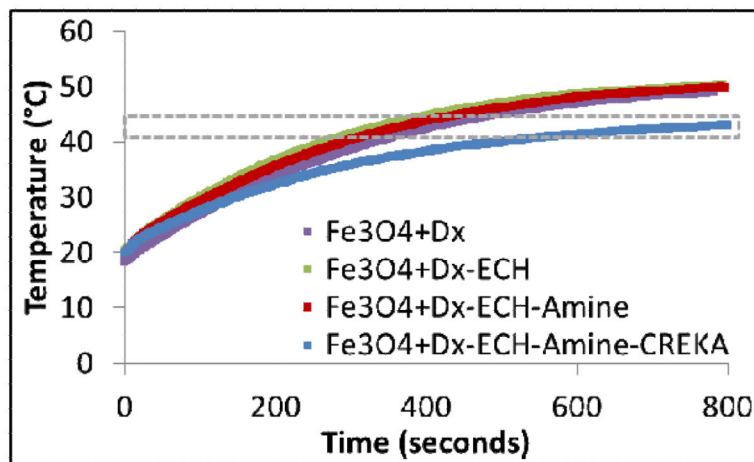


**Figure 5.**

Heating profiles of each nanoparticle system in the synthesis process (5 mg/mL Fe<sub>3</sub>O<sub>4</sub>) in the presence of an alternating magnetic field at 58 kA/m and 292 kHz (n = 3). The gray box indicates the target hyperthermia range.

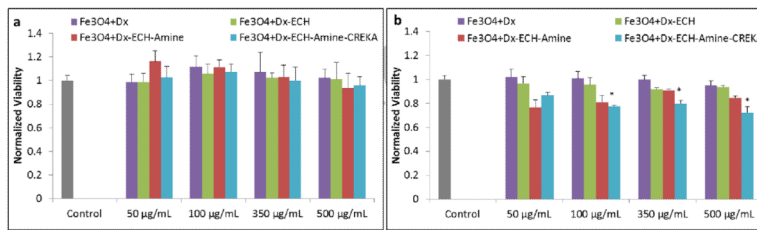


**Figure 6.**

Normalized viability of each nanoparticle system in the synthesis process on A549 lung cancer cells after (a) 24 hours of exposure and (b) 48 hours of exposure. Error bars represent standard error (n = 4) and \* indicates a significant difference (p < 0.05) using a 1-way ANOVA test.

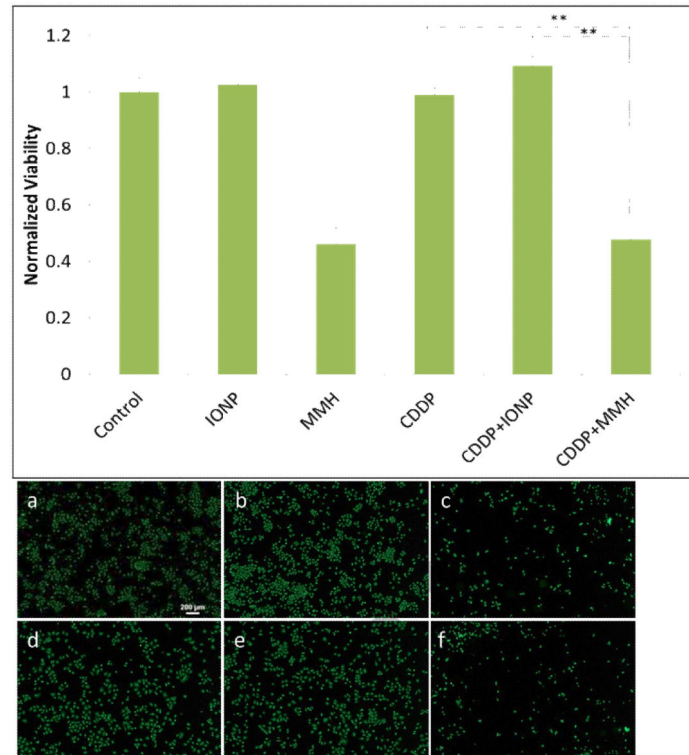


**Figure 7.**

Relative viability of A549 lung cancer cells 48 hours post magnetically mediated hyperthermia treatment. Error bars represent standard error (n = 12) and \*\* indicates a significant difference (p < 0.01). Representative images of A549 cells stained with calcein AM after 48 hours for: (a) Control, (b) IONP, (c)MMH, (d) CDDP, (e) CDDP+IONP, and (f) CDDP+MMH.

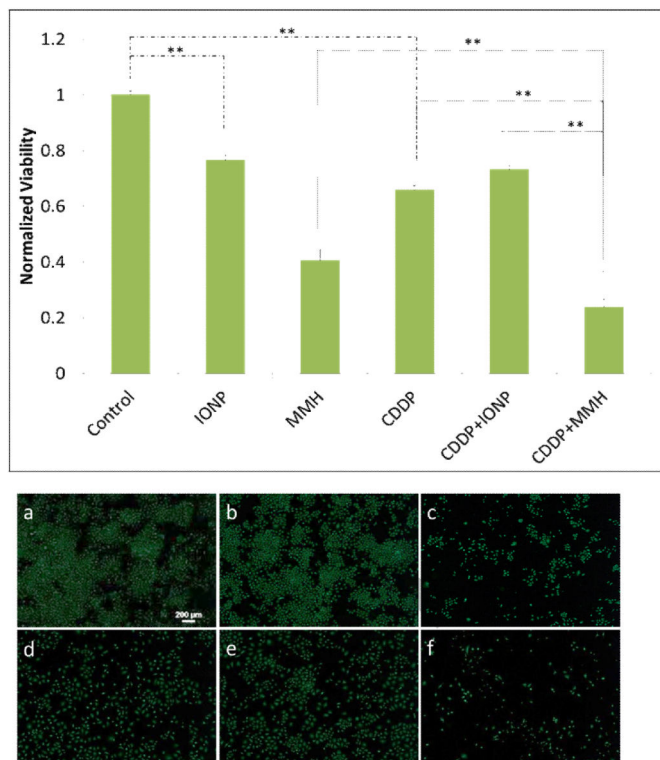


**Figure 8.**

Relative viability of A549 lung cancer cells 72 hours post magnetically mediated hyperthermia treatment. Error bars represent standard error with n = 12 and \*\* indicates a significant difference (p < 0.01). Representative images of A549 cells stained with calcein AM after 72 hours for: (a) Control, (b) IONP, (c) MMH, (d) CDDP, (e) CDDP+IONP, and (f) CDDP+MMH.

**Table 1**

Nanoparticle systems synthesized and characterized and their abbreviations, size as analyzed via DLS, and SAR values from AMF heating. Size of Fe<sub>3</sub>O<sub>4</sub>+Dx-ECH-Amine-CREKA via DLS could not be completed due to fluorescent tag but minimal difference from the other systems is expected.

Nanoparticle System	Abbreviation	Size (nm)	SAR (W/g)
Dextran coated IONP	Fe <sub>3</sub> O <sub>4</sub> +Dx	52 ± 16	81 ± 19
Epichlorohydrin crosslinked dextran coated IONP	Fe <sub>3</sub> O <sub>4</sub> +Dx-ECH	56 ± 11	98 ± 16
Amine-conjugated crosslinked dextran coated IONP	Fe <sub>3</sub> O <sub>4</sub> +Dx-ECH-Amine	52 ± 8	89 ± 9
CREKA-conjugated dextran coated IONP (CREKA-IONP)	Fe <sub>3</sub> O <sub>4</sub> +Dx-ECH-Amine-CREKA	---	66 ± 18

**Table 2**

Magnetically mediated hyperthermia treatments and controls.

Treatment	Description
Control	Media only
IONP	3 mg/mL Fe <sub>3</sub> O <sub>4</sub> (Fe <sub>3</sub> O <sub>4</sub> +Dx-ECH)
MMH	3 mg/mL Fe <sub>3</sub> O <sub>4</sub> plus 30 minutes AMF exposure
CDDP	100 μM cisplatin
CDDP+IONP	100 μM cisplatin plus 3 mg/mL Fe <sub>3</sub> O <sub>4</sub>
CDDP+MMH	100 μM cisplatin plus 3 mg/mL Fe <sub>3</sub> O <sub>4</sub> and 30 minutes AMF exposure

**Table 3**

Bound-to-free fluorescence for each system to fibrin clots represented by average  $\pm$  standard error (n = 4).

System	Bound-to-free fluorescence
CREKA only	0.69* $\pm$ 0.03
CREKA-IONP	0.62* $\pm$ 0.03
FITC-IONP	0.42 $\pm$ 0.04

The \* indicates a significant difference from the FITC-IONP bound-to-free fluorescence ratio ( $p < 0.05$ ).